

# RSC Advances



This is an *Accepted Manuscript*, which has been through the Royal Society of Chemistry peer review process and has been accepted for publication.

*Accepted Manuscripts* are published online shortly after acceptance, before technical editing, formatting and proof reading. Using this free service, authors can make their results available to the community, in citable form, before we publish the edited article. This *Accepted Manuscript* will be replaced by the edited, formatted and paginated article as soon as this is available.

You can find more information about *Accepted Manuscripts* in the [Information for Authors](#).

Please note that technical editing may introduce minor changes to the text and/or graphics, which may alter content. The journal's standard [Terms & Conditions](#) and the [Ethical guidelines](#) still apply. In no event shall the Royal Society of Chemistry be held responsible for any errors or omissions in this *Accepted Manuscript* or any consequences arising from the use of any information it contains.

## Correlation between hardness and pressure of CrB<sub>4</sub>

Y. Pan<sup>1</sup>, Y.H. Lin<sup>1,\*</sup>, M. Wen<sup>2</sup>, Q.N. Meng<sup>2</sup>

<sup>1</sup>School of Materials Science and Engineering, Southwest Petroleum University, Chengdu 610500, PR China

<sup>2</sup>Department of Materials Science, Key Laboratory of Automobile Materials of MOE and State Key Laboratory of Superhard Materials, Jilin University, Changchun 130012, PR China

\* E-mail address: [yhlin28@163.com](mailto:yhlin28@163.com) (Y.H. Lin).

### Abstract:

The correlation between hardness and pressure of CrB<sub>4</sub> with two different structures is investigated by first-principles approach. With increasing pressure, the hardness gradually decreases in contrast to bulk modulus, shear modulus, Young's modulus and B/G ratio monotonically increase. Pressure gives rise to hard transition from superhard to hard materials, which is in good agreement with experimental. Moreover, the pressure leads to brittle-to-ductile transition at 200 GPa based on the analysis of B/G ratio, which is consistent with the hard trend. The analysis of density of states and chemical bonding implies that pressure induces the electronic compression and collapse in localized region, and the variation of hardness is originated from the bond reversal between B-B (3) and B-B (2) covalent bonds, which located at the applied load plane. Finally, we conclude that the hardness of CrB<sub>4</sub> under pressure is related to the B/G ratio and bond characteristics.

### 1. Introduction

As the potential superhard materials, transition metal borides (TMBs) have attracted attention due to the high hardness, high elastic modulus, ultra-incompressibility, good thermal stability and metallic behavior et al<sup>1-5</sup>. Some potential superhard materials such as ReB<sub>2</sub> (48 GPa)<sup>6</sup>, WB<sub>4</sub> (46.2 GPa)<sup>7</sup>, OsB<sub>2</sub> (35.2 GPa)<sup>8</sup> and RuB<sub>2</sub> (36.1 GPa)<sup>8</sup> have been proposed and investigated intensively in recent years. Theoretical calculations show that the high hardness derives from B-B and TM-B covalent bonds. Especially, the 3D-network covalent bonds improve resistant to deformation and enhance hardness. However, there has been considerable controversy about the measured hardness and applied load. Latini et al<sup>9</sup> reported that the measured hardness of RuB<sub>2</sub>, RhB<sub>1.1</sub>, ReB<sub>2</sub> and IrB<sub>1.35</sub> rapidly decreases with increasing applied load. They found that the hard trend is, the higher the applied load, the lower the hardness for TMBs. For example, the measured hardness of ReB<sub>2</sub> at 0.49 N is 49.9

GPa and the measured value is only about of 20.8 GPa at 9.81 N<sup>10</sup>. Obviously, the hard feature of TMBs is strongly related to the applied load. In particular, could the TMBs are superhard materials? Unfortunately, the correlation between hardness and applied load remains elusive whether experimental or theoretical calculation.

Recently, CrB<sub>4</sub> is of great interest due to the high shear modulus, high hardness and metallic behavior et al. The calculated shear modulus of CrB<sub>4</sub> is 312 GPa<sup>11</sup>, which is obvious higher than that of diborides such as ReB<sub>2</sub> (267 GPa)<sup>12</sup>, OsB<sub>2</sub> (168 GPa)<sup>13</sup> and RuB<sub>2</sub> (184 GPa)<sup>14</sup> et al. This tetraboride has been synthesized by Niu et al<sup>15</sup>. They found that the measured hardness is 48 GPa under ambient pressure condition, and defined its structure as an orthorhombic structure (space group: *Pnnm*, No: 58), which is slightly different from previous structure (space group: *Immm*, No: 71) with  $a = 4.744 \text{ \AA}$ ,  $b = 5.477 \text{ \AA}$  and  $c = 2.866 \text{ \AA}$ , while the Cr and B atoms occupy the sites  $2a(0, 0, 0)$  and  $8c(0.175, 0.345,$

0), respectively<sup>16</sup>. The structural model of CrB<sub>4</sub> is shown in Fig. 1. Our previous work shown that the hardness of this structure originates from the B-B bonds cage, while the bond cage in this structure is composed of 12 boron atoms and the Cr atom is located at the center of B12 cage<sup>17</sup>. Therefore, this bond states with 3D-network bonds will improve the resistance to shape and shear deformation.

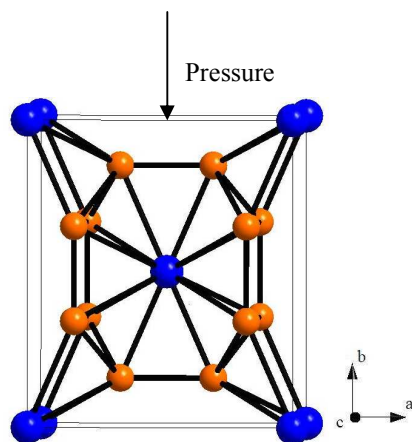


**Fig. 1.** The structural model of CrB<sub>4</sub>, The blue and brown spheres represent the Cr and B atoms, respectively.

As we know, the Vickers hardness of a solid is related to the load stress,  $P$  and the indentation  $d$  according to the Vickers hard principle<sup>6, 18</sup>. We suggest that the applied load plane of Vickers hardness is in the  $a$ - $c$  plane and the direction of applied load is the  $b$ -direction. The pressure along the  $b$ -direction is equal to the applied load (see Fig. 1). To investigate the correlation between hardness and applied load, in the present paper, we have used the first-principles approach to study the structural information, elastic modulus, hardness and electronic structure of CrB<sub>4</sub> with two different structures under high pressure. This paper is organized as follows: firstly, we describe the calculation method. Secondly, we represent the obtained results and discussion of CrB<sub>4</sub> under high pressure. Finally, we give a brief conclusion.

## 2. Methods

To study the mechanical properties under

pressure, two different structures of CrB<sub>4</sub> were considered in this paper. All structural optimizations were performed at pressures between 0 GPa and 400 GPa. Structural information, elastic modulus, hardness and electronic structure were carried out with the density functional theory (DFT) using the CASTEP code<sup>19</sup>. The exchange correlation functional was treated by local density approximation (LDA) with the Ceperley-Alder (CA)<sup>20</sup>. The valence electron configuration of Cr and B atoms is the  $3p^63d^54s^1$  and  $2s^22p^1$ , respectively. The interaction between ions and electrons was described through the ultra-soft pseudopotential<sup>21</sup>. A plane-wave basis set for electron wave function with cut-off energy of 400 eV was used. Integrations in the Brillouin zone were performed by using special  $k$ -point generated with  $7 \times 7 \times 12$  for these structures. During the structural optimization, no symmetry and no restriction were constrained for unit-cell shape, volume and atomic position. The structural relaxation was stopped until the total energy, the max force, the max stress and the max displacement were less than  $1 \times 10^{-5}$  eV/atom, 0.001 eV/Å, 0.03 GPa and 0.001 Å, respectively. To investigate the electronic structure, the actual spacing of DOS calculation was less than  $0.015 \text{ \AA}^{-1}$ , and the  $k$ -point generated by DOS was  $10 \times 9 \times 17$  Monkhorst-Pack grids.

## 3. Results and discussion

Hardness of a material indicates the resistance to elastic strain and plastic deformation. In general, superhard material is defined as  $H_v \geq 40 \text{ GPa}$ <sup>22</sup>. To estimate the micro-hardness ( $H_v$ ) of CrB<sub>4</sub> under pressure, the hard equation is given by<sup>23</sup>:

$$H_v = 2 \cdot (k^2 \cdot G)^{0.585} - 3 \quad (1)$$

where  $k$  represents the shear modulus vs bulk modulus and  $G$  is the shear modulus, respectively.

Fig. 2 shows the calculated theoretical

hardness of CrB<sub>4</sub> with two different structures as a function of pressure. Here, the calculated theoretical hardness of CrB<sub>4</sub> with *Pnnm* and *Immm* structures at zero pressure is 53.5 GPa and 48.5 GPa, respectively. The theoretical hardness of CrB<sub>4</sub> with *Immm* structure is lower than that of *Pnnm* structure, which is close to experimental result<sup>15</sup>. As we know, the *Pnnm* and *Immm* belong to the orthorhombic structure. Therefore, we suggest that the hard discrepancy derives from atomic arrangement in CrB<sub>4</sub>. Moreover, the theoretical hardness of CrB<sub>4</sub> gradually decreases with increasing pressure whether *Pnnm* structure or *Immm* structure. There is no doubt that the initial pressure results in elastic deformation. However, the strong B-B covalent bonds indeed create a significant resistance to follow the plastic flow to pin the dislocation. The decreasing of hardness under low pressure is more rapidly than hardness under high pressure. Finally, the crystal structure is damaged and the material is to break down under pressure. It is worth to notice that the hardness is lower than 40 GPa when the pressure of *Pnnm* and *Immm* structures above 70 GPa and 90 GPa, respectively. Therefore, we conclude that pressure leads to hard transition from superhard to hard materials.

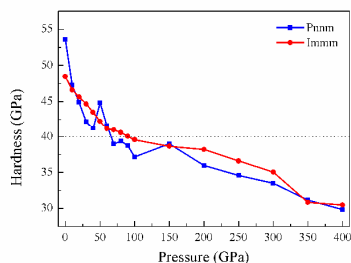


**Fig. 2.** Calculated theoretical hardness of CrB<sub>4</sub> as a function of pressure.

To reveal the relationship between hardness and pressure, the structural information, elastic modulus, bond characteristics and electronic structure should be analyzed and discussed, here. Fig. 3 displays the calculated lattice parameters

of CrB<sub>4</sub> with *Pnnm* and *Immm* structures as a function of pressure. The calculated lattice parameters of CrB<sub>4</sub> with *Pnnm* structure are  $a=4.644 \text{ \AA}$ ,  $b=5.400 \text{ \AA}$ ,  $c=2.801 \text{ \AA}$  and  $a/c=0.603$ , which are in good agreement with the previous experimental results and theoretical data<sup>15, 24</sup>. The calculated lattice parameters of CrB<sub>4</sub> with *Immm* structure are  $a=4.671 \text{ \AA}$ ,  $b=5.414 \text{ \AA}$ ,  $c=2.805 \text{ \AA}$  and  $a/c=0.601$ , which are in good agreement with the previous results<sup>16, 17, 25</sup>. We found that the lattice parameters of *Pnnm* structure are slightly smaller than that of *Immm* structure. Like most TMBs, CrB<sub>4</sub> exhibits lattice contraction under high pressure, and the calculated lattice parameters,  $a$ -axis,  $b$ -axis and  $c$ -axis monotonically decrease with increasing pressure. In particular, the variation of  $a/c$  ratio for *Immm* structure is bigger than that of *Pnnm* structure, reflecting the increasing isotropic interatomic potential under pressure. On the other hand, these results indicate that the localized hybridization between Cr and B atoms along the  $c$ -axis is stronger than  $a$ -axis under pressure, which is an important finding because it validates the isotropic force potential used in theoretical model for elastic modulus. This variation is further demonstrated by bond characteristics (see Fig. 8).

The structural stability is estimated by formation enthalpy, and the formation enthalpy of CrB<sub>4</sub> can be calculated by:

$$\Delta H(\text{CrB}_4) = E_{\text{total}}(\text{CrB}_4) - E_{\text{Cr}} - 4E_{\text{B}} \quad (2)$$

where  $E_{\text{total}}(\text{CrB}_4)$ ,  $E_{\text{Cr}}$  and  $E_{\text{B}}$  are the total energy of CrB<sub>4</sub>, pure Cr and B atoms at ground state, respectively.

The calculated formation enthalpy of CrB<sub>4</sub> with *Pnnm* and *Immm* structures as a function of pressure is plotted in Fig. 4. As we know, the formation enthalpy of a solid strongly depends on the electronic chemical potential and the atomic chemical potentials. The negative formation enthalpy indicates the thermodynamic stable. From Fig. 4, the calculated formation

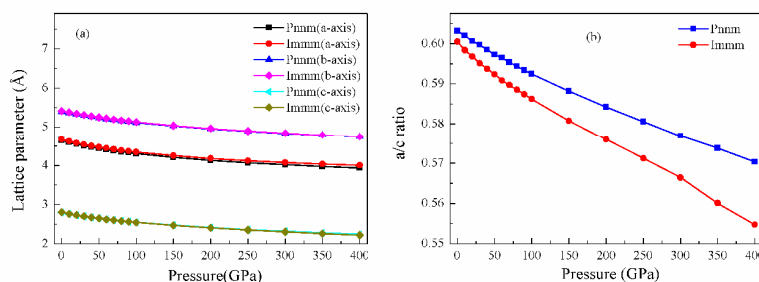


**Fig. 3.** Calculated lattice parameters of  $\text{CrB}_4$  as a function of pressure. (a) Lattice parameters vs pressure, (b) *a/c* ratio vs pressure.

enthalpy of *Pnmm* and *Immm* structures under zero pressure is  $-8.620$  eV/atom and  $-8.584$  eV/atom, respectively. Namely, the formation enthalpy of *Pnmm* structure is lower than that of *Immm* structure by  $0.036$  eV/atom, indicating that the former is more stable than the latter, which is in good agreement with experimental. However, it is obvious that the formation enthalpy of  $\text{CrB}_4$  monotonically increases as pressure increases over the entire pressure regime studied. There is no doubt that pressure leads to lattice distortion and finally damages its crystal structure.

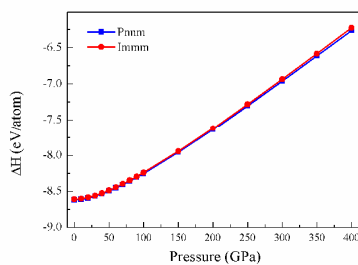


**Fig. 4.** Calculated formation enthalpies of  $\text{CrB}_4$  as a function of pressure.

The elastic modulus of a solid is very important because they check the mechanical stability, hardness, strength, Debye temperature and brittle or ductile behavior et al. In general, the elastic modulus includes bulk modulus, shear modulus and Young's modulus. The bulk modulus means the resistance to shape

deformation and the shear modulus indicates the resistance to shear deformation. Young's modulus provides a measure of stiffness of a material, while the higher the Young's modulus, the stronger the stiffer. According to the Pugh rule<sup>26</sup>, the ductile or brittle behavior of a solid is determined by B/G ratio. The critical value which separates ductile and brittle materials has been evaluated to be equal to 1.75. If  $B/G > 1.75$ , a solid exhibits ductile behavior in contrast to  $B/G < 1.75$ , the material in a brittle manner. In fact, the value of B/G ratio is related to the hard trend. The general trend is, the lower the B/G ratio, the higher the hardness for a material<sup>17</sup>. Therefore, the B/G ratio trend indirectly reflects the hardness. In this paper, the calculated elastic modulus is adopted by Voigt-Reuss-Hill (VRH) approximation according to the structural symmetry<sup>27</sup>.

Fig. 5 represents the bulk modulus, shear modulus and Young's modulus of  $\text{CrB}_4$  with *Pnmm* and *Immm* structures as a function of pressure. It can be seen that the calculated bulk modulus, shear modulus and Young's modulus of  $\text{CrB}_4$  with *Pnmm* structure under zero pressure is 275 GPa, 284 GPa and 634 GPa, respectively, which are in good agreement with the previous theoretical results<sup>24</sup>. Meanwhile, the calculated bulk modulus, shear modulus and Young's modulus of  $\text{CrB}_4$  under zero pressure is 295 GPa, 282 GPa and 642 GPa, respectively, which are in

excellent agreement with the previous theoretical results<sup>25</sup>. Obviously, the bulk and Young's modulus of *Immm* structure are bigger than that of *Pnmm* structure in contrast to shear modulus for former is lower than the latter. We presume this discrepancy may be due to the atomic configuration in  $\text{CrB}_4$  and shows why the theoretical hardness of *Pnmm* structure is different from the *Immm* structure.

Moreover, the bulk modulus, shear modulus and Young's modulus increase linearly with increasing pressure. For example, the calculated bulk modulus, shear modulus and Young's modulus of *Immm* structure at 400 GPa is 1495 GPa, 651 GPa and 1705 GPa, while the bulk modulus, shear modulus and Young's modulus at 400 GPa is 5.07, 2.31 and 2.66 times higher than zero pressure. It is understandable that pressure leads to localized hybridization between atoms, which gives rise to lattice distortion and has high elastic modulus. It is to be mentioned that the increasing velocity of bulk and Young's modulus is larger than that of shear modulus, meaning that the resistance to shape deformation is stronger than the resistance to shear deformation under pressure.

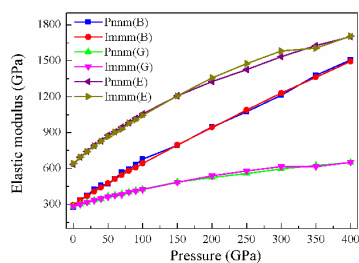
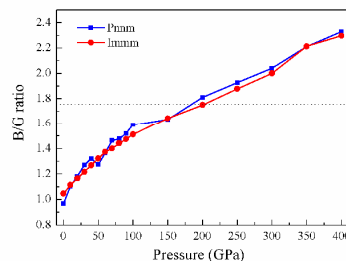


**Fig. 5.** Calculated elastic modulus of  $\text{CrB}_4$  as a function of pressure.

Over the past decades, the hardness of a material is measured by bulk and shear modulus, which can be obtained according to the first-principles approach<sup>28, 29</sup>. They pointed out that the bigger bulk and shear modulus of a solid has high hardness. Comparing the Fig. 2 and Fig.

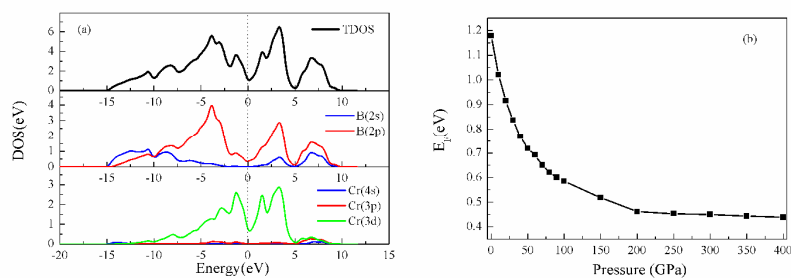
5, we found that the variation of elastic modulus deviates from the hard trend. In other words, the hardness of TMBs is not determined by bulk and shear modulus in this boride. Therefore, we suggest that the hardness of  $\text{CrB}_4$  is estimated by other factors such as B/G ratio and covalent bonds et al.

Fig. 6 shows the B/G ratio of  $\text{CrB}_4$  with *Pnmm* and *Immm* structures as a function of pressure from zero pressure to 400 GPa. The calculated B/G ratios of *Pnmm* and *Immm* structures at zero pressure is 0.968 and 1.046, respectively, which are smaller than that of  $\text{ReB}_2$  (1.254)<sup>30</sup>. For *Pnmm* and *Immm* structures, the obtained B/G ratios between zero pressure and 200 GPa are smaller than 1.75, indicating that  $\text{CrB}_4$  exhibit brittle behavior and have high hardness. However, we note that the B/G ratios increase gradually with increasing pressure. The calculated B/G ratios from 200 GPa to 400 GPa are bigger than 1.75, and the obtained B/G ratios of *Pnmm* and *Immm* structure are 2.329 and 2.296 at 400 GPa, respectively. There is no doubt that pressure results in brittle-to-ductile transition from brittle to ductile behavior and the hardness becomes lower under pressure, which is consistent with the variation of hardness. Therefore, we conclude that the hard trend of  $\text{CrB}_4$  under pressure is estimated by B/G ratio.



**Fig. 6.** Calculated B/G ratio of  $\text{CrB}_4$  as a function of pressure.

The structural stability and bond characteristics of  $\text{CrB}_4$  with pressure are demonstrated by electronic structure. Fig. 7 represents the density of states (DOS) and the



**Fig. 7.** (a) Calculated total and partial density of states (DOS) of CrB<sub>4</sub> under zero pressure, (b) the value of  $E_F$  as a function of pressure.

value at Fermi level ( $E_F$ ), with respect to the pressure, while the black vertical dashed of DOS represents  $E_F$ . Clearly, the DOS profile shows that the CrB<sub>4</sub> exhibits metallic behavior because some bands cross  $E_F$ . Just below  $E_F$ , the DOS profile is mainly contributed by Cr-3d state, B-2s state and B-2p state, reflecting the significant hybridization between Cr and B atoms, and forms the Cr-B covalent bonds. In addition, the strong hybridization between B and B atoms forms B-B covalent bonds.

Although the DOS profiles with pressure near  $E_F$  remain almost unchanged, the value at  $E_F$  decreases gradually with increasing pressure. The result indicates that the hybridization between atoms becomes stronger. On the other hand, the deep valley at  $E_F$  called “pseudogap” separates the bonding and antibonding regions. The pseudogap in PDOS affirms the existence of directional covalent bond, and can effectively resistance to elastic and plastic deformation. However, with increasing pressure, the pseudogap becomes narrower, implying strong hybridization between electronic orbits. Therefore, the decreasing of  $E_F$  under pressure results in electronic compression and collapse in small region and finally destroys the crystal structure.

In order to unravel the hard nature associated with the pressure, we examine the bond distances of different covalent bonds and

Mulliken's population of CrB<sub>4</sub> with *Immm* structure under pressure. Fig. 8 shows the calculated Cr-B and B-B covalent bonds with corresponding Mulliken's population as a function of pressure. As seen in Fig. 1 and Fig. 8 (c), the bond feature of CrB<sub>4</sub> is composed of B-B (1) covalent bond along the *b*-axis, B-B (2) covalent bond, B-B (3) covalent bond along the *a*-axis and the Cr-B bond is located at the center of B-B bond cage. The calculated covalent bonds: B-B (1), B-B (2), B-B (3) and Cr-B under zero pressure are 1.706 Å, 1.796 Å, 1.829 Å and 2.068 Å, respectively. The calculated bond length of B-B covalent bonds is shorter than that of Cr-B bond and the bond length of B-B (1) covalent bond is shorter than that of B-B (2) and B-B (3) covalent bonds. On the other hand, the Mulliken's population with positive and negative values indicate bonding and antibonding states, respectively, while the bigger the positive value, the stronger the bond covalency. A value of Mulliken's population close to zero means that there is no significant interaction between atoms. The calculated results show that the value of Mulliken's population of B-B (1), B-B (2), B-B (3) and Cr-B under zero pressure is 0.90, 1.55, 0.44 and -0.16, respectively. These results imply that the Cr-B bond exhibits antibonding state and the hybridization between B atoms along *b*-axis is stronger than other directions.

Considering the Vickers hard principle and

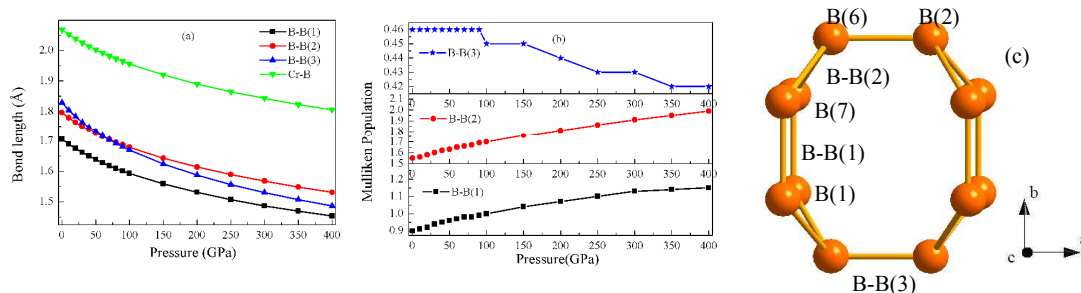


**Fig. 8.** (a) Bond lengths of B-B and Cr-B covalent bonds as a function of pressure, (b) Mulliken Population of B-B covalent bonds as a function of pressure, (c) B-B bond cage.

bond characteristics of  $\text{CrB}_4$ , we suggest that the Vickers hardness of  $\text{CrB}_4$  is determined by B-B (3) and part of B-B (2) covalent bonds. As pressure increases, the bond length of Cr-B and B-B covalent bonds becomes shorter. Moreover, the bond length of B-B (2) covalent bond below 70 GPa is shorter than that of B-B (3) covalent bond in contrast to bond length for former above 70 GPa is bigger than the latter. On the other hand, Fig. 8 (b) shows that the values of Mulliken's population of B-B (1) and B-B (2) covalent bonds gradually increase with increasing pressure. These results illustrate that pressure enhances the localized hybridization between B-B (1) and B-B (2) covalent bonds. However, we note that the value of Mulliken's population of B-B (3) covalent bond remains unchanged below 90 GPa and the value of Mulliken's population of B-B (3) covalent bond decreases when pressure above 90 GPa. Although the bond length of B-B (3) covalent bond becomes short, the localized hybridization between B-B (3) covalent bond becomes weak under pressure. Based on the analysis of bond length and Mulliken's population, pressure weakens the bond strength of B-B (3) and B-B (2) covalent bonds compared with the B-B (1) covalent bonds. Therefore, we suggest that pressure causes the deformation and finally fracture along the weak B-B (3) and B-B (2) covalent bonds. There is a main reason why the

$\text{CrB}_4$  has large hard discrepancy with pressure.

#### 4. Conclusion

In summary, we have presented first-principles density functional theory to investigate the structural stability, formation enthalpy, hardness, elastic modulus, brittle-to-ductile transition and bond characteristics of  $\text{CrB}_4$  from 0 GPa to 400 GPa. *Pnmm* and *Immm* structures are considered in this paper. The calculated theoretical hardness of *Pnmm* and *Immm* structures under zero pressure is 53.5 GPa and 48.5 GPa, respectively, and obtained lattice parameters, bulk modulus and shear modulus at zero pressure are in good agreement with the previous experimental results and theoretical data. Pressure leads to the electronic compression and collapse in localized region and the structure becomes unstable based on formation enthalpies. As pressure increases, the hardness gradually decreases, which the existence of hard transition from superhard to hard materials. On the contrary, the bulk modulus, shear modulus and Young's modulus linearly increase. The calculated B/G ratio shows that pressure results in brittle-to-ductile transition, which is consistent with the hard trend. The hard variation is determined by B-B bond cage, while the B-B (3) and B-B (2) covalent bonds in *a-c* plane become weak compared with the B-B (1) covalent bond along the direction of applied load.

### Acknowledgments

Financial support by the National Natural Science Foundation of China (Grant No. 50525204) and the Important Natural Science Foundation of Yunnan (Grant No.2009CD134) are gratefully acknowledged.

### References

- 1 R. W. Cumberland, M. B. Weinberger, J. J. Gilman, S. M. Clark, S. H. Tolbert, R. B. Kaner, *J. Am. Chem. Soc.*, 2005, **127**, 7264.
- 2 B. J. Suh, X. Zong, Y. Singh, A. Niazi, D. C. Johnston, *Phys. Rev. B*, 2007, **76**, 144511.
- 3 L. Petr, C. X. Qiu, P. Raimund, *Phys. Rev. B*, 2009, **80**, 012103.
- 4 W. J. Zhao, Y. X. Wang, *J. Solid State Chem.*, 2009, **182**, 2880.
- 5 E. Deligoz, K. Colakoglu, Y. O. Ciftci, *Chin. Phys. B*, 2012, **21**, 106301.
- 6 H. Y. Chung, M. B. Weinberger, J. B. Levine, A. Kavner, J. M. Yang, S. H. Tolbert, R. B. Kaner, *Science*, 2007, **316**, 436.
- 7 Q. F. Gu, G. Krauss, W. Steurer, *Adv. Mater.*, 2008, **20**, 3620.
- 8 A. Šimůnek, *Phys. Rev. B*, 2007, **75**, 172108.
- 9 A. Latini, J. V. Rau, R. Teghil, A. Generosi, V. R. Alberini, *Appl. Mater. Inter*, 2010, **2**, 581.
- 10 A. Latini, L. V. Rau, D. Ferro, R. Teghil, V. R. Albertini, S. Barinov, *Chem. Mater.*, 2008, **20**, 4507.
- 11 H. B. Xu, Y. X. Wang, V. C. Lo, *Phys. Status. Solidi-R*, 2011, **5**, 13.
- 12 J. B. Levine, J. B. Betts, J. D. Garrett, S. Q. Guo, J. T. Eng, A. Migliori, R. B. Kaner, *Acta Mater.*, 2010, **58**, 1530.
- 13 H. Y. Gou, L. Hou, J. W. Zhang, H. Li, G. F. Sun, F. M. Gao, *Appl. Phys. Lett.*, 2006, **88**, 221904.
- 14 X. F. Hao, Y. H. XU, Z. J. Wu, D. F. ZHou, X. J. Liu, J. Meng, *J. Alloys. Compd.*, 2008, **453**, 413.
- 15 H. Y. Niu, J. Q. Wang, X. Q. Chen, D. Z. Li, Y. Y. Li, P. Lazar, *Phys. Rev. B*, 2012, **85**, 144116.
- 16 S. Andersson, T. Lundstrom, *Acta Chem. Scand.*, 1968, **22**, 3103.
- 17 Y. Pan, W. T. Zheng, W. M. Guan, K. H. Zhang, X. F. Fan, *J. Solid State Chem.*, 2013, **207**, 29.
- 18 J. A. Rau, A. Latini, *Chem. Mater.*, 2009, **21**, 1407.
- 19 M. D. Segall, P. J. D. Lindan, M. J. Probert, C. J. Pickard, P. J. Hasnip, S. J. Clark, M. C. Payne, *J. Phys-condens. Mat.*, 2002, **14**, 2717.
- 20 D. M. Ceperley, B. J. Alder, *Phys. Rev. Lett.*, 1980, **45**, 566.
- 21 D. Vanderbilt, *Phys. Rev. B*, 1990, **41**, 7892.
- 22 Y. Zhang, H. Sun, C. F. Chen, *Phys. Rev. B*, 2006, **73**, 064109.
- 23 X. Q. Chen, H. Y. Niu, D. Z. Li, Y. Y. Li, *Intermetallics.*, 2011, **19**, 1275.
- 24 B. Li, H. Sun, C. Zang, C. Chen, *Phys. Rev. B*, 2013, **87**, 174106.
- 25 X. Y. Chong, Y. H. Jiang, R. Zhou, J. Feng, *J. Alloys. Compd.*, 2014, **610**, 684.
- 26 S. F. Pugh, *Philos Mag A*, 1954, **45**, 823.
- 27 R. Hill, *Proc. Phys. Soc. A*, 1952, **65**, 349.
- 28 F. Gao, *Phys. Rev. B*, 2006, **73**, 132104.
- 29 Y. X. Wang, *Appl. Phys. Lett.*, 2007, **91**, 101904.
- 30 Y. Pan, W. T. Zheng, W. M. Guan, K. H. Zhang, S. S. Yu, X. Y. Hu, *Comput Mater Sci*, 2014, **82**, 12.

